Experimental Demonstration of 128×128 Optical Cross-Connects with 2.45 Pbps Throughput

Takuro Ochiai(1), Takuma Kuno(1), Ryuji Munakata(1), Yojiro Mori(1), Shih-Chun Lin(2), Motoharu Matsuura(3), Suresh Subramaniam(4), Hiroshi Hasegawa(1)

(1) Nagoya University, hasegawa@nuee.nagoya-u.ac.jp
(2) North Carolina State University
(3) University of Electro-communications
(4) George Washington University

Abstract *We experimentally demonstrate 128×128 optical cross-connects with 2.45 Pbps throughput. Numerical simulations confirm routing penalty of around 1% for various metro and core network topologies. Transmission experiments using the full extended C-band clearly show its applicability to metro and core networks.*

Introduction

The network capacity must be increased to handle the rapidly growing network traffic. The fibre-capacity improvement attained by enhancing the spectral efficiency is now reaching the theoretical limit [1]. To offset this limit, space-division multiplexing (SDM) technologies utilizing multiple single-core fibres (SCFs) or multi-core fibres (MCFs) are being extensively studied [2,3]. In attaining such systems, the high core parallelism of SDM-based networks requires high-port-count optical cross-connects (OXCs) to bridge the numerous cores of optical fibres installed on each link [4-8]. The typical OXC used in present SCF-based networks comprises multiple wavelength selective switches (WSSs) [9]. A 1×95 WSS prototype has been reported so far [10]; however, the port count of commercially available WSSs is still limited to around 50 [11,12]. As a result, the OXC port count attained with such WSSs is also limited to around 50. This motivates us to develop a novel OXC architecture that attains port expandability necessary for future large-capacity networks.

To realize the high-port-count OXC in a practical way, we have proposed an OXC architecture that can be configured only with commercially available mature devices, i.e., low-port-count splitters/WSSs and high-port-count matrix switches [13]. This OXC architecture has routing restriction of contention; however, our contention-aware routing algorithm based on graph degeneracy can make the routing penalty marginal. Our previous work proved that the routing performance degradation relative to ideal all-WSS-based nodes, which need numerous high-port-count WSSs and thus are infeasible, is less than 2%. A proof-of-concept transmission experiments using a 16×16 OXC prototype with 300.8 Tbps throughput was reported in OFC2023 [13].

In this paper, we demonstrate a 128×128 OXC by conducting transmission experiments using 32-Gbaud DP-QPSK and DP-16QAM signals aligned in the full extended C-band. The net throughput reaches 1.22 Pbps with QPSK signals and 2.45 Pbps with 16QAM signals. Numerical simulations on several metro and core network topologies show the good routing performance with marginal penalty. The good transmission characteristics thanks to our low-loss architecture were also confirmed; the transmissible distances were 3100 km for QPSK signals and 700 km for 16QAM signals.

High-port-count OXC Architecture

Fig. 1 depicts N×N OXCs based on (a) broadcast-and-select (B&S) architecture and (b) route-and-select (R&S) architecture [8,14]. The B&S architecture comprises N 1×(N+1) splitters and N (N+1)×1 WSSs whereas the R&S architecture comprises N 1×(N+1) WSSs and N (N+1)×1 WSSs. If N is larger than ~10, the B&S OXC cannot be realized due to the excessive power loss yielded by high-degree splitters. If N is larger than ~50, we need to cascade or parallelize multiple small-port-count WSSs to create a single large-port-count WSS; this architecture is infeasible in most cases as too many costly WSSs and optical amplifiers are necessary [15].

Fig. 2 illustrates an N×N OXC based on our proposed architecture, where N 1×(B+1) splitters, B N×N matrix switches, and N (B+1)×1 WSSs are connected. The operation principle is as follows: the splitter distributes an optical signal to the following matrix switches, where one of the output ports of the splitter is used for dropping signals. Then, the matrix switch delivers the signal to the WSS connected to the target output port. After that, the WSS selectively combines the input signals, where one of the input ports of the WSS is used for adding signals. This architecture

https://doi.org/10.1049/icp.2023.2536

has colourless and directionless routing capability thanks to the wavelength selectivity of the WSSs and full connectivity of matrix switches. Although this architecture has contention on optical-path routing, the penalty can be suppressed by using a contention-aware routing algorithm based on graph degeneracy [13].

The remarkable benefit of adopting this OXC architecture is its scalability. As shown in the next section, a reasonable value of B in Fig. 2 is 3. Therefore, we can construct, as one example, a 128×128 OXC with 1×4 splitters, 128×128 matrix switches, and 4×1 WSSs; all of these devices are commercially available.

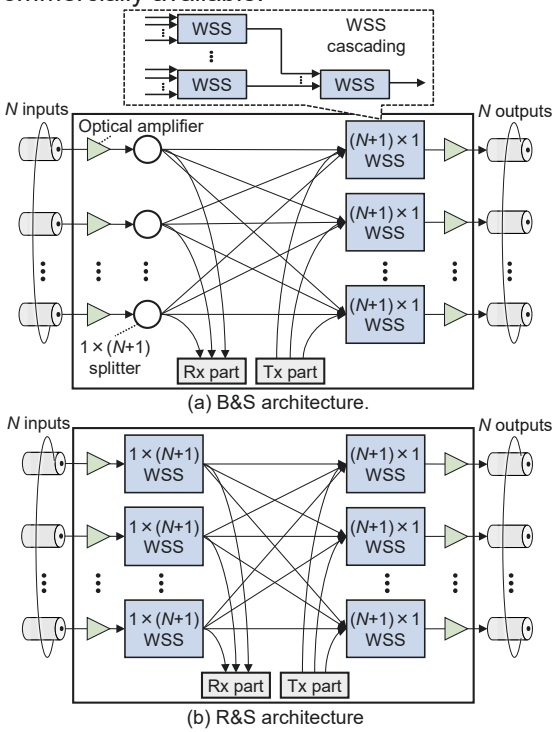

Fig. 1: Conventional OXC architectures.

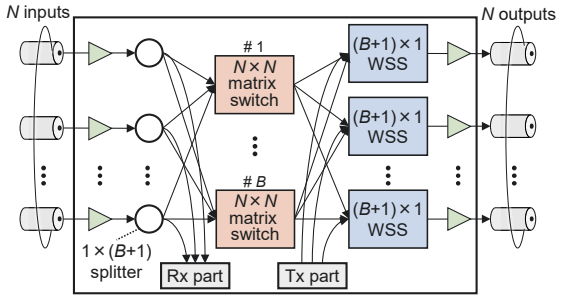

Fig. 2: Proposed OXC architecture, where $B < N$.

Simulations on Routing Performance

We newly examine two core-network topologies and two metro-network topologies as summarized in Tab. 1 [16-19]. The available frequency range of each fibre is set to 4.8 THz assuming the full extended C-band, i.e., 384 12.5 GHz frequency slots are utilized. Traffic demands are generated as a set of optical path setup requests, where the source and destination nodes are uniformly and randomly selected. To assess the system, we employ the traffic intensity metric, which is defined by the average number of optical paths connecting every pair of nodes. We consider three distinct optical path categories, with each path requiring 4, 7, or 15 frequency slots. The occurrence probability of each path category is assigned a value of 1/3. We adopt our contention-aware routing algorithm based on graph degeneracy [13]. The baseline architecture is the ideal all-WSS-based node though it is impractical for OXC port counts greater than 50; this OXC can route any input wavelength to any output port with the exception being wavelength contention on a fibre. Each result is obtained by averaging the results of 20 calculations.

Fig. 3 shows the number of necessary fibres calculated against traffic intensity, where the results are normalized by baseline performance. When the traffic intensity is low, the increase in the number of fibres is large. This is because the number of accessible adjoining nodes is small when the number of fibres connected to nodes is small. Here, let us focus on the high-traffic-intensity region that corresponds to the target situation in this paper; by setting B = 3, the fibre increment incurred is around 1% for all network topologies. Thus, we can utilize commercially available 4×1 WSSs to construct the OXC even though the OXC port count exceeds 100.

Tab. 1: Network topologies.

					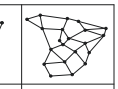
Network topology		US LATA	Verizon	German	Spanish
Number of nodes		11	14	17	21
Number of links		23	19	26	35
Node degree	Max.	8	5	6	4
	Min.	2	2	2	2
	Ave.	4.18	2.71	3.06	3.33

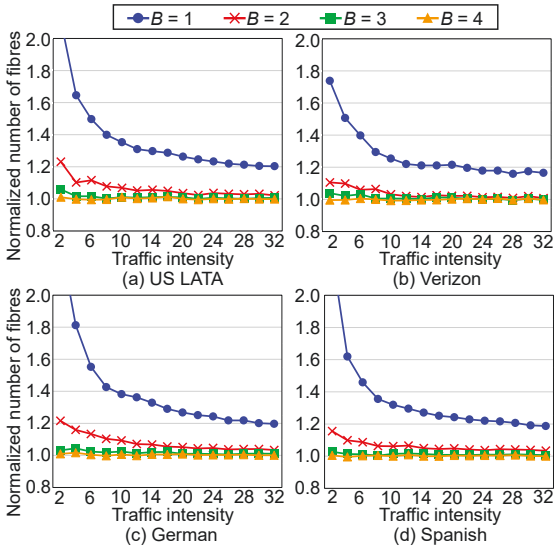

Fig. 3: The normalized number of fibres vs. traffic intensity, where B+1 is the degree of splitters/WSSs.

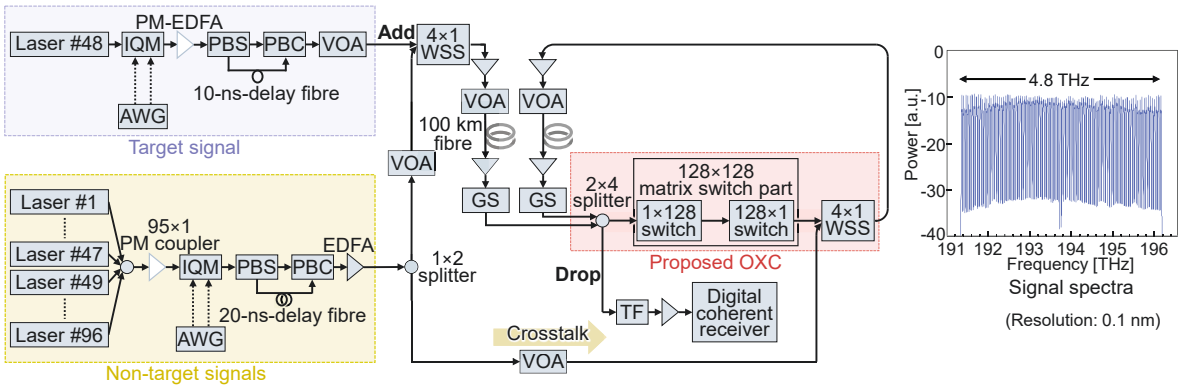

IQM	IQ modulator	WSS	Wavelength selective switch
AWG	Arbitrary waveform generator	GS	Gate switch
EDFA	Erbium-doped fibre amplifier	TF	Tuneable filter
PM-EDFA	Polarization maintaining EDFA	PBS	Polarization beam splitter
VOA	Variable optical attenuator	PBC	Polarization beam combiner

Fig. 4: Experimental configuration.

Experiments on Transmission Characteristics

To confirm the feasibility of our OXC architecture, we conducted transmission experiments. Fig. 4 depicts the experimental system, where a part of the 128×128 OXC was constructed. A 32 Gbaud QPSK/16QAM signal was formed by an IQ modulator (IQM) driven by an arbitrary-waveform generator (AWG) with two output ports. The polarization-division multiplexing was emulated in a split-delay-combine fashion. After power adjustment using variable optical attenuators (VOAs), the target signal and 95-wavelength non-target signals were combined by a 4×1 WSS. The spectra of the 96-wavelength signals are shown in Fig. 4, where the signal powers were flattened within ±0.9 dB. After power optimization using a VOA, the signals were launched into a 100 km optical fibre with dispersion coefficient of 16.5 ps/nm/km, attenuation coefficient of 0.2 dB/km, and nonlinearity coefficient of 1.5 /W/km. Then, the signals were input to the loop transmission system that comprised a pair of synchronous gate switches (GSs), our proposed OXC, an erbium-doped fibre amplifier (EDFA) followed by a VOA, a 100 km fibre, and an EDFA. According to the simulation results shown in Fig. 2, we adopted B = 3, i.e., 1×4 splitter and 4×1 WSS were used to construct the OXC. The 128×128 OXC consisted of 2×4 coupler/splitter, part of 128×128 matrix switch, and 4×1 WSS. Note that 2×4 coupler/splitter has functions of the 2×2 coupler for the loop system and the 1×4 splitter for the OXC concurrently; the undesired excess loss due to the loop system was thus minimized. The matrix switch was based on microelectromechanical system (MEMS) whereas the WSS was based on liquid crystal on silicon (LCOS); both devices are widely utilized in real-world networks. The OXC loss was 17.1 dB in total. Here, we assumed the worst case in terms of filtering effect; the spectrum narrowing was induced at every OXC traversal. After traversing the loop system, the signal was dropped by the 2×4 coupler/splitter. The target signal was then extracted by a wavelength-tuneable filter and recovered by a digital coherent receiver.

Fig. 5 plots the BER measured against transmission distance or node hop count. We observe that 31 hops/3100 km and 7 hops/700 km can be transmitted using QPSK and 16QAM signals when the target BER was set considering forward error correction (FEC). These results clearly show that the proposed OXC architecture can be applied to most metro and core networks.

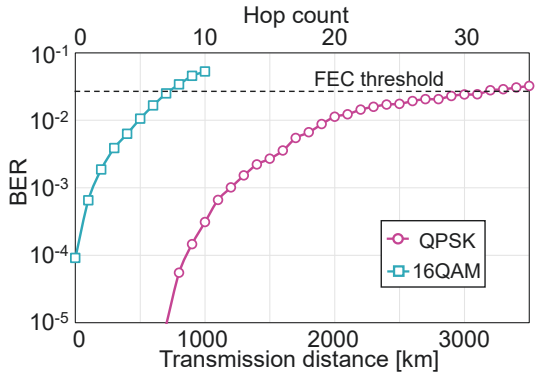

Fig. 5: Measured BER vs. transmission distance/hop count.

Conclusion

This paper demonstrated a 128×128 OXC with throughput of 2.45 Pbps, assuming its application to future high-capacity optical networks. Its feasibility was successfully confirmed through network simulations and transmission experiments. This architecture is fully extensible since matrix switches with size of over 300×300 are commercially available [20,21].

Acknowledgements

This research and development work was supported in part by NICT and NSF.

References

[1] R. Essiambre, G. Kramer, P. J. Winzer, G. J. Foschini, and B. Goebel, "Capacity limits of optical fiber networks," *Journal of Lightwave Technology*, vol. 28, no 4, pp. 662-701, 2010, DOI: 10.1109/JLT.2009.2039464.

[2] D. J. Richardson, J. M. Fini, and L. E. Nelson, "Space-division multiplexing in optical fibres," *Nature Photonics*, vol. 7, pp. 354-362, 2013, DOI: 10.1038/nphoton.2013.94.

[3] B. J. Puttnam, G. Rademacher, and R. S. Luís, "Space-division multiplexing for optical fiber communications," *Optica*, vol. 8, no 9, pp. 1186-1203, 2021, DOI: 10.1364/OPTICA.427631.

[4] D. M. Marom, P. D. Colbourne, A. D'Errico, N. K. Fontaine, Y. Ikuma, R. Proietti, L. Zong, J. M. Rivas-Moscoso, and I. Tomkos, "Survey of photonic switching architectures and technologies in support of spatially and spectrally flexible optical networking [Invited]," *Journal of Optical Communications and Networking*, vol. 9, no 1, pp. 1-26, 2017, DOI: 10.1364/JOCN.9.000001.

[5] P. J. Winzer, D. T. Neilson, and A. R. Chraplyvy, "Fiber-optic transmission and networking: the previous 20 and the next 20 years [Invited]," *Optics Express*, vol. 26, no 18, pp. 24190-24239, 2018, DOI: 10.1364/OE.26.024190.

[6] M. Jinno, "Spatial Channel Network (SCN): Opportunities and challenges of introducing spatial bypass toward the massive SDM era [Invited]," *Journal of Optical Communications and Networking*, vol. 11, no. 3, pp. 1-14, 2019, DOI: 10.1364/JOCN.11.000001.

[7] R. S. Luís, B. J. Puttnam, G. Rademacher, T. A. Eriksson, Y. Hirota, S. Shinada, A. Ross-Adams, S. Gross, M. Withford, R. Maruyama, K. Aikawa, Y. Awaji, H. Furukawa, and N. Wada, "Experimental demonstration of a petabit per second SDM network node," *Journal of Lightwave Technology*, vol. 38, no. 11, pp. 2886-2896, 2020, DOI: 10.1109/JLT.2020.2988886.

[8] T. Kuno, Y. Mori, S. Subramaniam, M. Jinno, and H. Hasegawa, "Design and evaluation of a reconfigurable optical add-drop multiplexer with flexible wave-band routing in SDM networks," *Journal of Optical Communications and Networking*, vol. 14, no. 4, pp. 248-256, 2022, DOI: 10.1364/JOCN.450504.

[9] S. Gringeri, B. Basch, V. Shukla, R. Egorov, and T. J. Xia, "Flexible architectures for optical transport nodes and networks," *IEEE Communications Magazine*, vol. 48, no. 7, pp. 40-50, 2010, DOI: 10.1109/MCOM.2010.5496877.

[10] K. Suzuki, Y. Ikuma, E. Hashimoto, K. Yamaguchi, M. Itoh and T. Takahashi, "Ultra-high port count wavelength selective switch employing waveguide-based I/O frontend," in *Procedings Optical Fiber Communications Conference (OFC)*, Los Angeles, USA, 2015, DOI: 10.1364/OFC.2015.Tu3A.7.

[11] Lumentum, "TrueFlex twin 1×35 wavelength selective switch," https://www.lumentum.co.jp/ja/products/trueflex-twin-1x35-wavelength-selective-switch, accessed on 5 May 2023.

[12] Finisar, "Flexgrid twin 1x48 wavelength selective switch," https://www.globenewswire.com/news-release/2021/10/04/2307857/0/en/Finisar-Australia-Releases-the-World-s-First-Flexgrid-Twin-1x48-Wavelength-Selective-Switch.html, accessed on 5 May 2023.

[13] R. Munakata, T. Kuno, Y. Mori, S. Lin, M. Matsuura, S. Subramaniam, and H. Hasegawa, "Architecture and performance evaluation of bundled-path-routing multi-band optical networks," in *Proceedings Optical Fiber Communications Conference (OFC)*, San Diego, USA. 2023. DOI: Not available.

[14] S. L. Woodward, M. D. Feuer, and P. Palacharla, "ROADM-node architectures for reconfigurable photonic networks," Chapter 15 in *Optical Fiber Telecommunications VIB* edited by I. P. Kaminow, T. Li, and A. E. Willner, *Academic Press*, 2013, DOI: 10.1016/B978-0-12-396960-6.00015-8.

[15] M. Niwa, Y. Mori, H. Hasegawa, and K. Sato, "Tipping point for the future scalable OXC: What size M × M WSS is needed?," *Journal of Optical Communications and Networking*, vol. 9, no. 1, pp. A18-A25, 2017, DOI: 10.1364/JOCN.9.000A18.

[16] S. Kim and S. S. Lumetta, "Addressing node failures in all-optical networks," *Journal of Optical Networking*, vol. 1, no. 4, pp. 154-163, 2002, DOI: Not available.

[17] G. Welbrock, "Metro 100G applications and technology," *Optical Fiber Communications Conference (OFC) Market Watch Panel IV*, 2013, DOI: Not available.

[18] R. Hülsermann, S. Bodamer, M. Barry, A. Betker, C. Gauger, M. Jäger, M. Köhn, J. Späth, "A Set of Typical Transport Network Scenarios for Network Modelling," *5th ITG-Workshop on Photonic Networks*, pp. 129-136, 2004, DOI: Not available.

[19] O. Pedrola, L. Velasco, A. Castro, J. Fernández-Palacios, D. Careglio, and G. Junyent, "CAPEX study for grid dependent multi-layer IP/MPLS-over-EON using relative BV-WSS costs," in *Proceedings Optical Fiber Communications Conference (OFC) / National Fiber Optic Engineers Conference (NFOEC)*, Los Angeles, USA, 2012, DOI: Not available.

[20] Calient, "Calient's optical circuit switch," https://www.calient.net/wp-content/uploads/2022/06/Datasheet_Calients-Optical-Circuit-Switches.pdf, accessed on 5 May 2023.

[21] Polatis, "Polatis 576: 576x576 port software-defined optical circuit switch," https://www.polatis.com/polatis576.asp, accessed on 5 May 2023.